

## **Physico-chemical properties of Alanine-Sodium nitrate: An optical overview**

E. Gallegos-Loya and Duarte-Moller

### **Abstract**

Single crystals of the semi organic materials L-Alanine sodium nitrate (LASN) and D-Alanine sodium nitrate (DASN) were grown from an aqueous solution by slow evaporation technique. X-ray diffraction (XRD), studies were carried for the doped grown crystals. The absorption of these grown crystals was analyzed using UV-vis-NIR studies, and it was found that these crystals possess minimum absorption from 200 to 1100 nm. An infrared (FTIR) spectrum of single crystal has been measured in the 4000 400  $\text{cm}^{-1}$  range. The assignment of the observed vibrational modes to corresponding symmetry type has been performed. A thermo gravimetric study was carried out to determine the thermal properties of the grown crystal. The efficiency of second harmonic generation was obtained by a variant of the Kurtz-Perry method.

Key words: Nonlinear optical, second harmonic generation, Alanine sodium nitrate.

### **Introduction**

Nonlinear optics has emerged as one of the most attractive fields of current research in view of its vital applications in areas such as optical modulation, optical switching, optical logic, frequency shifting, and optical data storage for the developing technologies in telecommunication and signal processing (Anandha and Ramasamy, 2009). Extensive studies have been made on the synthesis and crystal growth of nonlinear optical (NLO) materials (Uma et al., 2008).

Semiorganic materials possess several attractive properties such as high NLO coefficient, high laser damage threshold and wide transparency range, high mechanical

strength and thermal stability, which make the materials suitable for second harmonic generation (SHG) and other NLO applications (Shethuraman et al., 2008).

Organic materials have been of particular interest because the NLO responses in this broad class of materials in microscopic origin, offers an opportunity to use theoretical modeling coupled with synthetic flexibility to design and produce novel materials (Uma et al., 2008).

Amino acids are the potential candidates for optical second harmonic generation (SHG) because they contain chiral carbon atom and crystallize in noncentro symmetric space groups (Praveen et al., 2008). A series of studies on semiorganic aminoacid compounds such as L-arginine phosphate (LAP), L-arginine hydrobromide (L-AHBr), L-histidine tetrafluoroborate (L-HFB) (Shethuraman et al., 2008) L-arginine hydrochloride (L-AHCl), (Meera et al., 2004) L-alanine acetate (L-AA) (Mohan et al., 2005) and glycine sodium nitrate (GSN) (Narayan and Dharmaparakash, 2002) as potential NLO crystals have been reported. Alanine is an amino acid which forms a number of compounds on reaction with inorganic acid and salts to produce an outstanding material for NLO applications (Shethuraman et al., 2008). The compound was first crystallized by Bernal and later by Simpson et al. It belongs to the orthorhombic crystal system (space group P212121) with a molecular weight of 89.09 and has a melting point of 297°C (Vijayan et al., 2006).

The compounds, L-alanine sodium nitrate and D-alanine sodium nitrate were obtained as the product by reaction of sodium nitrate and the amino acids L-alanine and D-alanine in aqueous solution. In the present investigation, single crystals were grown and characterized by X-ray diffraction powder, Fourier transform infrared (FTIR)

spectroscopic studies, Thermo gravimetric analysis (TGA/DTA), UV-Vis-NIR spectral analysis and the efficiency of second harmonic generation (SHG).

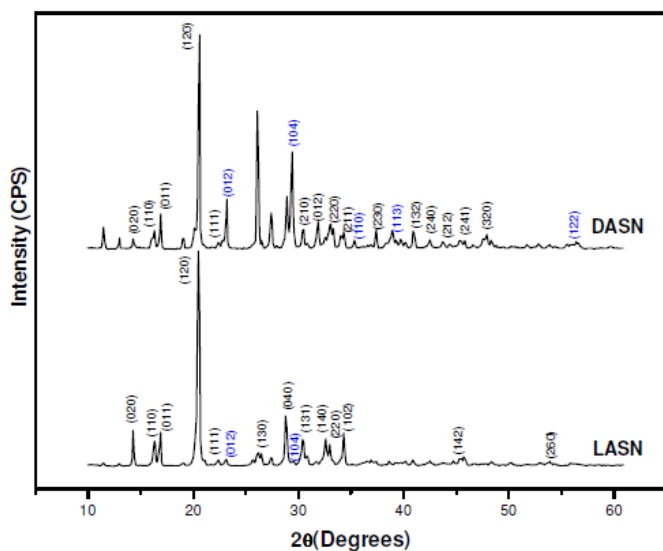


**Figure 1.** Powder X-ray diffractogram of L-alanine sodium nitrate (LASN) and D-alanine sodium nitrate (DASN).

## Experimental design

The crystals obtained during the development of this work were grown by slow evaporation technique at room temperature through an aqueous solution. The reactive commercially available L-alanine and D-alanine  $C_3H_7NO_2$  were used with stoichiometry Sigma-Aldrich Lab with 98% purity and molecular weight 89.09 g/mol and the sodium nitrate  $NaNO_3$  stoichiometry Sigma-Aldrich Lab with 99.9% purity and molecular weight 84.99 g/mol. The samples were prepared using 1:1 molar ratio in distilled water and constant agitation for 35 min and a temperature of 60°C. The evaporation time for the L-alanine sodium nitrate solution at room temperature was 45 days and 60 days for the D-alanine solution.

The Phillips Expert powder X-ray diffractometer with Cu K $\alpha$  radiation ( $\lambda = 1.5428$  Å) was used for the powder X-ray diffraction pattern. The sample was scanned in the  $2\theta$  values ranging from 10 to 60 at the rate of  $0.05^\circ/\text{min}$ .

In order to analyze the presence of functional groups, FTIR spectrum was recorded in the range of  $400\text{ cm}^{-1}$  to  $4000\text{ cm}^{-1}$  using a MAGNO IR 750 series II NICOLET spectrometer. The samples were added to a matrix of KBr to perform this procedure.

The UV-vis spectra gave limited information about the structure of the molecule because the absorption of UV and visible light involves promotions of the electrons in the  $\sigma$  and  $\pi$  orbitals from the ground state to higher energy states. The transition spectrum is very important for any NLO material because it can be of practical use only if it has a wide transparency window. NLO materials have a practical use only if they have a wide transparency state. To find this absorbance window, a Lambda 10 Perkin Elmer UV-Vis spectrometer was used. The scanning was done in the range of 200 to 1100 nm the same way as with the FTIR.

TGA/DTA was done in a TA Instruments STD 2960 Simultaneous DTA-TGA. The samples were heated from room temperature to more than  $1000^\circ\text{C}$  at rate of  $10^\circ\text{C}/\text{min}$ .

In order to find the SHG, the crystals were grown according to the Kurtz and Perry technique (Lydia et al., 2009) into powder (about  $70\text{ }\mu\text{m}$ ) and densely packed between two transparent microscope glass slides (Kurtz and Perry, 1968; Silverstein and Webster, 1998). Once the samples were placed into the glass slides, a Nd:YAG Quanta ray INDI series laser of 1064 nm generating an 8 ns pulse and operated at 6 mJ/pulse and at rate of 10 Hz is pumped at the proper angle and distance in order to

see SHG on green color (532 nm) that corresponds to the expected emitted light and it is the half wavelength of the incoming light.

### X-ray diffraction

The resultant peaks in the diffractogram (Figure 1) show an intense peak at  $20.54^\circ$ , which coincides with the plane (120) and the reflections of the planes (020), (110), (040), (140), (111), (220), (102), (131), (142) and (260), corresponding to the principal planes of the L-alanine present in the L-alanine sodium nitrate, where the planes (012) and (104) were identified with nitrate. The peaks appearing in the spectrum that have not been identified can be attributed to the formation of the L-alanine sodium nitrate compound. In both the L-alanine and D-alanine cases, the presence of an intense peak at  $20.59^\circ$  which coincides with the plane (120) and reflections from planes (020), (110), (011), (111), (210), (012), (220), (211), (230), and (241), corresponding to the principal planes of the D-alanine present in the D-alanine sodium nitrate was identified. The planes (012) (104) (110) (113) and (122) were identified with nitrate. The peaks appearing in the spectrum that have not been identified can be attributed to the formation of the compound D-alanine sodium nitrate.

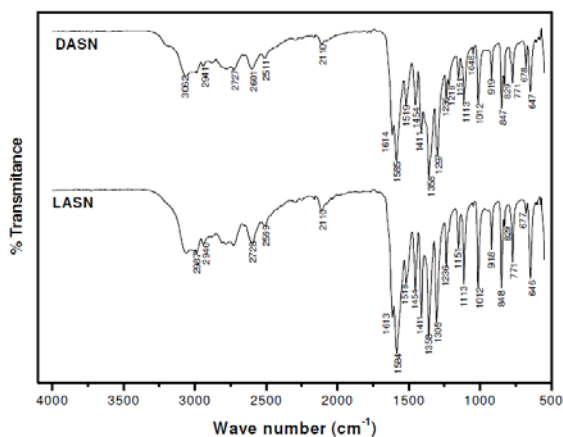


Figure 2. FTIR spectrum of LASN and DASN.

## FT-IR study

In order to obtain the presence of functional groups, FTIR spectrum was recorded in the range of  $400\text{ cm}^{-1}$  to  $4000\text{ cm}^{-1}$  by using a MAGNO IR 750 series II NICOLET spectrometer.

The sample of L-alanine sodium nitrate (LASN) and D-alanine sodium nitrate (DASN) were added to a matrix of KBr to perform this procedure as shown in Figure 2. The presence of the carboxyl acid group around  $3000\text{ cm}^{-1}$  can be observed due to the Alanine presence. The main internal vibrations of Alanine are observed on the functional groups ( $\text{NH}_3^+$ ,  $\text{CH}_2$ ,  $\text{COO}^-$ ) which is in agreement with the data reported before (Lydia et al., 2009); symmetric and asymmetric bending vibrations were observed on the  $\text{CH}_3$  groups for LASN and DASN at  $2987$  and  $1454\text{ cm}^{-1}$ . The peak at  $2599$  and  $2601\text{ cm}^{-1}$  is symmetrical stretching of CH to LASN and DASN respectively. The  $1151$ ,  $1218$  and  $1236\text{ cm}^{-1}$  frequencies are attributed to the rocking deformation of the  $\text{NH}_3^+$  group (Meera et al., 2004). Furthermore the peak  $1048\text{ cm}^{-1}$  is a symmetrical stretching of CCN group.

Other low frequency bands are typical for  $\text{N-H}\cdots\text{O}$  Hydrogen bonds arising from the overtones around the  $2727\text{ cm}^{-1}$ . The rest of the functional groups:  $\text{COO}^-$ , CN and  $\text{NO}_3$  between  $500$  and  $1500\text{ cm}^{-1}$  also agree with the reported data.

Usually the presence of nitrates in the lattice can be identified by their characteristic signature in the ranges:  $1660$ - $1625$ ,  $1300$ - $1255$ ,  $870$ - $833$  and  $763$ - $690\text{ cm}^{-1}$  (Baran et al., 2003). Parent compound traces were identified in the synthesized compound. The presence of the  $\text{NO}_3$  group in the LASN and DASN can be identified by the peaks at  $1358$ ,  $1113$ ,  $849$  and  $771\text{ cm}^{-1}$ . The symmetric and asymmetric  $\text{NH}_3^+$

stretching vibrations appear at frequencies 2941 and 2110  $\text{cm}^{-1}$  respectively. The absorption peaks at 1613, 1584, and 1518  $\text{cm}^{-1}$  for LASN, and 1614, 1585 and 1519  $\text{cm}^{-1}$  for DASN confirm the presence of  $\text{NH}_3$  bending. The presence of nitro groups in the spectrum confirms the LASN and DASN compounds. Other important functional groups are detailed in Table 1.

### **Raman spectroscopy**

The Raman spectra were carried out at room temperature in frequency range 400-4000  $\text{cm}^{-1}$  with Xplora Raman microscope HORIBA system. The laser Raman spectrum, showing the presence of more intense peak around 850  $\text{cm}^{-1}$ , is due to  $\text{COO}^-$  stretching mode of vibrations (Figure 3). The peaks at 1113 and 1112  $\text{cm}^{-1}$  are assigned to  $\text{NO}_3$  stretching.

The C-H and N-H bending vibrations are observed at 1306  $\text{cm}^{-1}$  as a sharp peak. The asymmetric  $\text{CH}_3$  bending at 1422  $\text{cm}^{-1}$  and O-H bending is around 950  $\text{cm}^{-1}$  (Britto et al., 2008). The peak at 1411  $\text{cm}^{-1}$  is assigned to the symmetric stretching C-COO carboxyl group.

In Raman spectra of alanine, the symmetric and asymmetric deformation vibrations of the  $\text{NH}_3^+$  groups appear in the region between 1680–1470  $\text{cm}^{-1}$  (Baran and Ratajczak, 2006); in the spectrum L-alanine and Dalanine we found in 1531 y, 1939, 1659, 1630, 1599, 1596  $\text{cm}^{-1}$  frequency. The position of  $\text{NH}_3^+$  asymmetric stretching frequency, indicate the formation of intra and inter-molecular strong N-H---O hydrogen bonding of the  $\text{NH}_3^+$  group, with the oxygen of both the carbonyl group and inorganic nitrates (Hernández-Paredes, 2008; Vijayakumar et al., 2008).

**Table 1.** FT-IR and Raman functional group assignments of the grown LASN and DASN.

Raman ( $\text{cm}^{-1}$ )		FT-IR ( $\text{cm}^{-1}$ )		Assignments
LASN	DASN	LASN	DASN	
3706				Overtone
3426				Overtone
			3062	Symmetric $\text{CH}_3$ stretching
3000	3003			Asymmetric $\text{CH}_3$ stretching
		2987		Symmetric $\text{CH}_3$ stretching
2964	2964			$\text{CH}_2$ stretching and asymmetric $\text{CH}_3$ stretching
2948				Symmetric $\text{CH}_2$ stretching
		2941	2941	Symmetric $\text{NH}_3$ stretching
2936	2933			Asymmetric $\text{CH}_2$ stretching
2888	2888			$\text{CH}_2$ stretching
	2734			Overtone
		2728	2727	N-H....O and O-H....O stretching
	2603		2601	Symmetric CH stretching
		2599		Symmetric CH stretching
			2511	Overtone
2512				Overtone
2484				Overtone
2444	2442			Overtone
		2251		$\text{CH}_3$ stretching
2123	2119			Overtone
		2110	2110	Asymmetric $\text{NH}_3$ stretching
1939				Asymmetric $\text{NH}_3$ deformation
1775				Asymmetric $\text{COO}^-$ stretching
1659				Asymmetric $\text{NH}_3$ deformation
1630				Asymmetric $\text{NH}_3$ deformation
		1613	1614	$\text{NH}_3$ bending
1599	1596			Asymmetric $\text{NH}_3$ deformation
		1584	1585	$\text{NH}_3$ bending
1571				Asymmetric $\text{COO}^-$ stretching
	1543			Overtone
1531				Symmetric $\text{NH}_3$ deformation
		1518	1519	$\text{NH}_3$ bending
1503				$\text{CH}_3$ deformation
	1496			Overtone
1486	1489			Asymmetric $\text{COO}^-$ deformation
1466	1465			$\text{C}_6\text{H}_2$ scissors mode
		1454	1454	Asymmetric $\text{CH}_3$ bending
1422				$\text{CH}_3$ bending
	1412	1411	1411	Symmetric C-COO <sup>-</sup> stretching
1386				$\text{CH}_3$ puckering
1363	1366			Wagging $\text{CH}_2$ deformation
		1358	1358	$\text{NO}_3$ stretching
	1312			$\text{CH}_2$ wagging
1306		1306		C-H and N-H bending
			1297	Flexed position $\text{CH}_2$
	1235	1236	1236	$\text{NH}_3^+$ Rocking
		1218	1218	$\text{NH}_3^+$ Rocking
1151	1150	1151	1151	$\text{NH}_3^+$ Rocking and symmetric $\text{COO}^-$ stretching
1113	1112	1113	1113	$\text{NO}_3$ stretching
1070				Overtone
1050		1048	1048	Symmetric CCN stretching



Table 1. Contd.

1022	1027			CH <sub>3</sub> rocking
		1012	1012	Overtone of torsional oscillation NH <sub>3</sub> <sup>+</sup>
926				NH <sub>3</sub> rocking
	936			CH <sub>2</sub> rocking
		918	919	Overtone of torsional oscillation NH <sub>3</sub> <sup>+</sup>
853	850			N-C stretching
		849	847	NO <sub>3</sub> stretching
		829	829	C-C stretching
774	774			OH deformation
		771	771	NO <sub>3</sub> stretching
725				COO wagging
		677	678	NO <sub>3</sub> <sup>-</sup> in plane deformation
	651	646	647	COO <sup>-</sup> in plane deformation
		578	578	Overtone

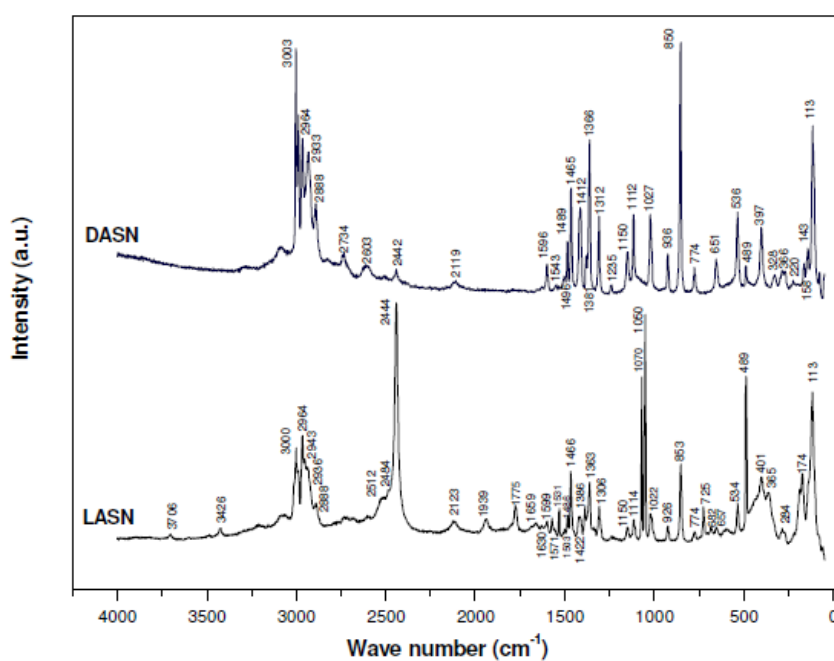


Figure 3. Raman spectrum of LASN and DASN.

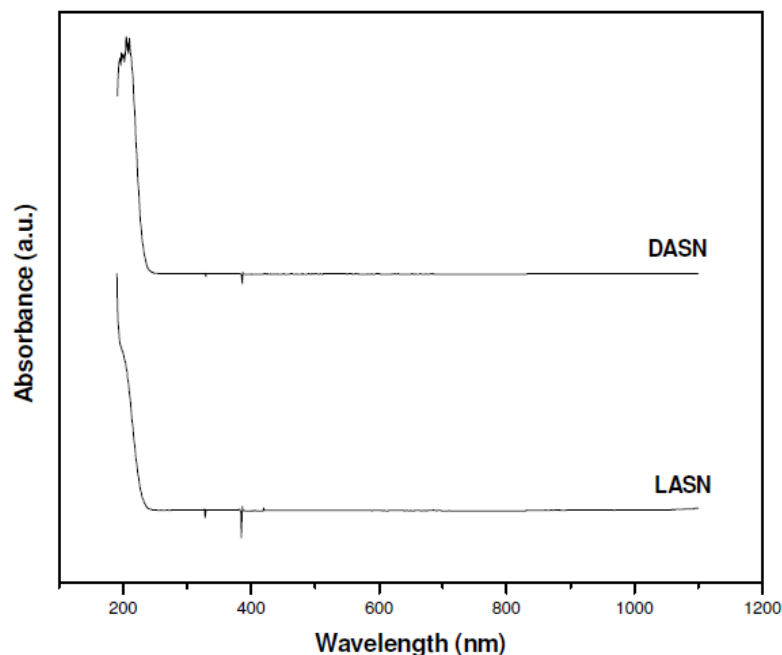


Figure 4. UV-vis spectra of the LASN and DASN.

The study of symmetry stretching and stretching vibration of  $\text{CH}_2$  group is observed in 2948 and 2964, 2888  $\text{cm}^{-1}$ . The band around 1235, 1150, 1151 and 926  $\text{cm}^{-1}$  is also indicative of the  $\text{NH}_3$  rocking modes. The peak at 1366  $\text{cm}^{-1}$  is a deformation of  $\text{CH}_2$  group, and at 1312  $\text{cm}^{-1}$  is attributed to the  $\text{CH}_2$  wagging. The intensity varies upon the source used for analyzing the sample. Other important functional groups are detailed in Table 1.

### UV-vis study

Figure 4 shows the absorbance zone above 250 nm (Ultra-violet wavelength) where a wide band completely transparent in all the visible range is observed (Infrared wavelengths) (Lydia et al., 2009; Martin and Natarajan, 2008; Ramesh et al., 2006). This means that this material presents a good non-absorbance band in the visible range for expected applications. A little protuberance around the 300 nm is observed (Narayan and Dharmaprakash, 2002; Narayan 2002). This little peak is still outside the visible

zone (UV zone) and it could present some absorbance if the crystal were to be excited with 600 nm (red color) trying to obtain a second harmonic of 300 nm (UV color). Other noticeable characteristic in the absorption spectrum is a wide transparency window within the range of 400–1100 nm which is desirable for NLO crystals because the absorptions in an NLO material near the fundamental or second harmonic signals will lead to the loss of the conversion of SHG. Due to this property, LASN and DASN have potential uses for SHG using an Nd: YAG laser (1064 nm) to emit a second harmonic signal within the green region (532 nm) of the electromagnetic spectra.

### Thermal analysis

Figure 5 shows the TGA pattern of the LASN and DASN showing good stability below 220°C with a rapid dropping beyond that temperature (Lydia et al., 2009; Ambujam et al., 2006). Figure 4 also shows the DTA pattern of LASN where an exothermic transition appears at about 230°C. Meanwhile, it is pure and presents another endothermic transition at 400°C (Lydia et al., 2009; Ambujam et al., 2006). Within this temperature range, the possible NLO applications becomes promising due to the use of laser powers, for LASN and DASN performing below 230°C.

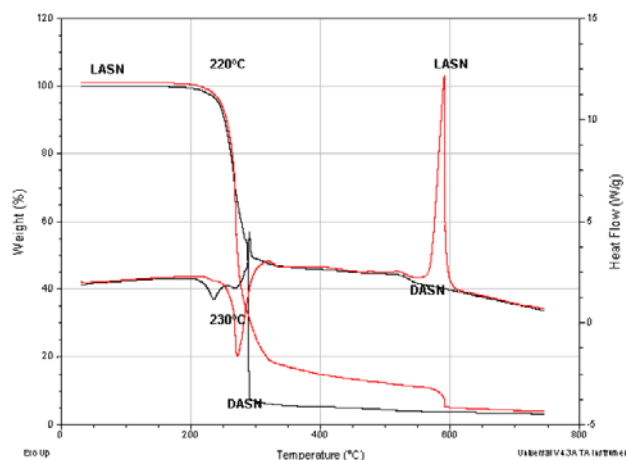


Figure 5. TGA and DSC curves of LASN and DASN.

## **SHG signal detection**

Figure 6 shows the data collected from the detector where the SHG signal is plotted vs the beam energy. This kind of experiments has been used in order to measure the damage threshold. In this case, the SHG intensity tends to increase when the beam energy is also increased. This experiment shows the good quality of these crystals for the second harmonic generation, but there is a better efficiency in the LASN sample.

## **Conclusions**

A new non-linear optical semiorganic crystal, LASN and DASN were synthesized. The single crystals were grown from an aqueous solution. Functional groups of good quality crystals of LASN and DASN grown by the slow evaporation technique have been detected by FTIR and Raman spectroscopies. Also based on UV-vis spectra observations, an absorption zone below the 250 nm (Ultra-violet wavelengths) can be seen recovering a good transmittance values across all the visible range until near IR frequencies and beyond. This situation shows these crystals can be used for applications involving the band of visible light. The transparency of the crystal in the visible and infrared regions shown in transmission spectra confirms the NLO property of this.

Other characterization was the thermal response. The TGA/DTA results show a degrading temperature about 230°C which promises to have good applications at high temperatures, revealing that the crystal is thermally stable until that temperature.

The SHG test is the first one performed in this kind of material and was observed that the SHG intensity tends to be directly proportional to the beam energy and follows a

linear tendency with a positive slope which promises to be a good non-linear optical material.

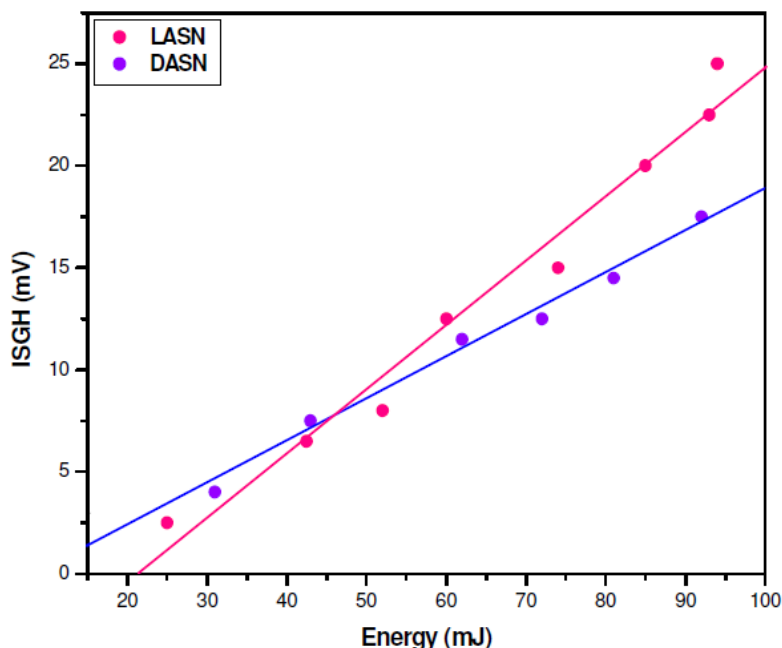


Figure 6. Linear fit for the SHG intensity as function of the beam energy.

Finally, we succeeded in obtaining good quality crystals of LASN and DASN and for the first time, the second harmonic generation was detected in this material which indicates that these crystals are new materials with nonlinear optical properties with potential applications.

### Acknowledgments

Authors thank the National Council of Science and Technology of Mexico for its financial support. Also to National Laboratory of Nanotechnology of CIMAV, S.C., at Chihuahua, Mexico. The authors are very grateful to Enrique Torres Moye (M. Sc) (X-ray Laboratory), Daniel Lardizabal (M. Sc) (Thermal Analysis Laboratory), Luis de la Torre (Uv-vis analysis) and Antonio Silva Molina (Raman study).

## References

Ambujam K, Selvakumar S, Prem A, Mohamed G, Sagayaraj P (2006). "Crystal growth, optical, mechanical and electrical properties of organic NLO material  $\gamma$ -glycine", Cryst. Res. Tech., 41: 671-677.

Anandha BG, Ramasamy P (2009). "Synthesis, crystal growth and characterization of novel semiorganic nonlinear optical crystal: Dichlorobis(l-proline)zinc(II)" Materials Chem. Phys., 113: 727-733.

Baran J, Drozd M, Pietrazko A, Trzebiatowska M, Ratajczak H (2003). "Crystal Structure and Vibrational Studies of Glycine-LiNO<sub>3</sub> and Glycine-NaNO<sub>3</sub> Crystals" Polish J. Chem., 77: 1561-1577.

Baran J, Ratajczak H (2006). "Polarised vibrational studies of the  $\alpha$ - glycine single crystal. Part I. Polarised Raman spectra—the Problem of effective local Raman tensors for the glycine zwitterions." Vibrational Spectroscopy, 43:125–139.

Britto M, Das SA, Natarajan S (2008). "Growth and characterization of DL-Alanine- A new NLO material from amino acid family", Materials Lett., 62: 2633-2636.

Hernandez-Paredes J (2008). "Band structure, optical properties and infrared spectrum of glycine–sodium nitrate crystal." J. Molecular Structure, 875: 295-301.

Kurtz SK, Perry TT (1968). "A Powder technique for the evaluation of nonlinear optical materials". J. Appl. Phys., 39: 3798-3813.

Lydia CM, Sankar R, Indirani RM, Vasudevan S (2009). "Growth, optical, thermal and dielectric studies of an amino acid organic nonlinear optical material: l-Alanine". Materials Chem. Phys., 114: 490-494.

Meera K, Muralidharan R, Dhanasekaran R, Prapun M, Ramasamy P (2004).  
“Growth of nonlinear optical material: L-arginine hydrochloride and its characterisation”.  
J. Crystal Growth, 263: 510-516.

Mohan Kumar R, Rajan Babu D, Jayaraman D, Jayavel R, Kitamura K (2005).  
“Studies on the growth aspects of semi-organic L-alanine acetate: a promising NLO  
crystal”. J. Crystal Growth, 275: 7.

Narayan Bhat M (2002). "Effect of solvents on the growth morphology and  
physical characteristics of nonlinear optical  $\gamma$ -glycine crystals." J. Crystal Growth, 242:  
245-252.

Narayan Bhat M, Dharmaprakash SM (2002). “Growth of nonlinear optical  $\gamma$ -  
glycine crystals”, J. Crystal Growth, 236: 376-380.

Narayan BM, Dharmaprakash SM (2002). "New nonlinear optical material:  
glycine sodium nitrate". J. Crystal Growth, 235: 511-516.

Praveen Kumar P, Manivannan V, Tamilselvan S, Senthil S, Victor Antony R,  
Sagayaraj P, Madhavan J (2008). “Growth and characterization of a pure and doped  
nonlinear optical L-histidine acetate single crystals”. Optics Communications, 281: 2989-  
2995.

Ramesh Kumar G, Gokul Raj S, Mohan R, Jeyavel R (2006). “Influence of  
Isoelectric pH on the Growth Linear and Nonlinear Optical and Dielectric Properties of  
L-Threonine Single Crystals”. Cryst. Growth Des., 6: 1308–1310.

Sethuraman K, Ramesh Babu R, Gopalakrishnan R, Ramasamy P (2008).  
“Synthesis, Growth, and Characterization of a New Semiorganic Nonlinear Optical  
Crystal: L-Alanine Sodium Nitrate (LASN)”. Crystal Growth Des., 8(6): 1863-1869.

Silverstein RM, Webster FX (1998). "Spectrometric Identification of Organic Compounds" (Sixth Edition), John Wiley Eastern and Sons Inc, Canada.

Uma Devi T, Lawrence N, Ramesh Babu R, Ramamurthi K (2008). "Growth and characterization of L-prolinium picrate single crystal: A promising NLO crystal", J. Cryst. Growth, 310: 116-123.

Vijayakumar T, Hubert Joe I, Reghunadhan CP, Nair B, Jayakumar VS (2008). "Non-bonded Interactions and its Contribution to the NLO activity of Glycine Sodium Nitrate - A Vibrational Approach." J. Molecular Structure, 887: 20-35.

Vijayan N, Rajasekaran S, Bhagavannarayana G, Ramesh Babu R, Gopalakrishnan R, Palanichamy M, Ramasamy P (2006). "Growth and Characterization of Nonlinear Optical Amino Acid Single Crystal: L-Alanine" Cryst. Growth Des., 6(11): 2441–2445.